ADVANCES IN MATERIALS SCIENCE, Vol. 22, No. 3 (73), September 2022

DOI: 10.2478/adms-2022-0011

Abdu Hussen Ali

Chemistry Department, College of Natural and Computational Sciences, Mekdela Amba University, P.O. BOX: 32, Ethiopia

Email: abdelmelik9@gmail.com

g-C_3N_4/ BIO–SYNTHESIZED SILVER NANOPARTICLE FOR FLUOROMETRIC BIO-SENSING OF ACETYLCHOLINESTERASE AND MALATHION

ABSTRACT

Malathion is widely used in agriculture due to their high efficiency as insecticides. They are very toxic hazardous chemicals to both human health and environment even at low concentration. The detection of pesticides (malathion) at the low levels developed by the environmental protection agency (EPA) still remains a challenge. A highly efficient fluorescent biosensor based on g-C_3N_4/AgNPs for AChE and malathion detection is successfully developed by impregnation method. The structural and morphological properties of the nanocomposites were characterized by using powder X-ray diffraction (XRD), fourier- transform infrared spectroscopy (FT-IR) and scanning electron microscopy (SEM). The analysis confirmed that there is a strong interfacial interaction between g-C_3N_4 and AgNPs. The fluorescent responses show an increase in intensity upon the additions of AChE which indicates that AChE as enzyme was hydrolyzing the substrate ACh, with the increase in oxidative electron as the preferred route of reaction. The developed OFF-ON sensor immobilizes by Actylcholestrase (AChE) and use as new probe for malathion detection. In the absence of malathion, AChE−g-C_3N_4/AgNCs exhibit high fluorescence intensity. However, the strong interaction of the basic sites to malathion, causes fluorescence quenching via static quenching and Ag form aggregation on the surface of g-C_3N_4. The experimental parameter such as pH of buffer (pH=6), concentration of acetylcholine (1 mM) and malathion (500 μM) were optimized. The sensor was also more sensitive with Stern-Volmer quenching constants (K_{SV}) of $3.48x10^{3}$ M^{-1}. The practical use of this sensor for malathion determination in Khat was also demonstrated. The obtained amount of malathion in Khat is 168.8 μM.

Keywords: *Actylcholestrase; AgNPs; biosensor; fluorescence quenching; malathion; nanoparticle*

INTRODUCTION

Food and Drug Administration (FDA) reports about 1045 chemicals as pesticide residues [1]. Pesticides are chemical substances applied to crops at various stages of cultivation and during the post-harvest storage of crops. Despite the wide-ranging benefits of using pesticides in agriculture, several incorrect applications can result in high and undesirable levels of the compounds in the produce that reaches consumers [2]. Among the many pesticides, organophosphate pesticides (Ops) which are widely used in agriculture due to their high efficiency as insecticides. They are very toxic hazardous chemicals to both human health and environment even at low concentration [3].

Malathion is one of the most commonly used organophosphates pesticides (OPs) to control insects in fruits, vines, vegetables, field crops, glasshouse crops and in forestry, water and air. It can enter into the body through skin, inhalation, even though the amount adsorbed well depend on where there the exposure occurs on the body. Acute symptoms of malathion poisoning at high doses include nausea, headache and tightness in the chest, unconsciousness, convulsions and a prolonged worsening illness [4].

The residue of these OPs in the natural environment also generates a lot of pollution problems because they act as inhibitors of acetylcholinesterase (AChE) an essential enzyme that catalysis in a very efficient way the hydrolysis of the neurotransmitter acetylcholine. The inhibition acetylcholine can disturb the transmission of nerve impulses of most animal beings [5]. AChE has regained great attention recently due to its association with Alzheimer's disease and other neurodegenerative diseases characterized by low ACh levels owing to catabolism by AChE [6]. Moreover, AChE is the primary target of inhibition by organophosphorus compounds such as nerve agents and pesticides; thus, public concern about the development of detection devices for effectively monitoring pesticides. The combination of enzymatic reactions with the various methods of monitoring enzymatic products has allowed the development of enzyme-based devices for sensitive and rapid determination of acetylcholine, AChE and its inhibitors [7].

Detection of acetylcholinesterase (AChE) enzyme and pesticides developed by the environmental protection agency (EPA) still remains a challenge. The most commonly used traditional techniques are chromatography including gas chromatography and high performance liquid chromatography [8], capillary electrophoresis, electrochemistry, mass spectrometry, FTIR detection and various spectroscopic methods, have already been employed to detect acetylcholinesterase (AChE) enzyme and pesticides in biological, environmental and pharmaceutical samples [9]. Some of the above methods are accurate and selective; however, these techniques have several disadvantages. They require relatively expensive instrumentation and high consumption of organic reagents. Therefore, they are becoming expensive, require long analysis time and necessitate highly trained personnel and inability to be used for continuous monitoring in the field [10].

An alternative to classical methods for detection of acetylcholinesterase (AChE) enzyme and OP pesticides is the design of optical sensors (colorimetric or fluorometric biosensors). One of the most convenient and simple means of chemical detection is the generation of an optical signal, for example, changes in absorption or emission bands of the fluorometric biosensor in the presence of the target analyte. Recently, these fluorometric sensing have received a lot of attention due to their high sensitivity, selectivity, simplicity, low-cost instrumentation and field-work applicability for detection of AChE and also pesticides (malathion). In particular, nanomaterials-based biosensor have shown great promise due to their large surface area, high surface reactivity, and strong adsorption capacity.

Therefore, the evolution of nanotechnology represents an ever-improving process in the design, discovery, novel utilization, and creation of artificial nano scale materials [11]. To meet the major challenges in environmental sustainability, these nanomaterials are stimulating various important practical applications in the environmental sector for intensively studied in biological and environmental analysis. The morphology, fabrication, and modification of novel nanomaterials allow for enhanced performance for environmental related applications [12]. Commonly, nanomaterials can be employed for development of AChE-based sensing devices due to nanomaterials are used as enzyme carriers for loading a large amount of AChE to enhance the detection signal [13], also act as peroxidase- or oxidase-like activities catalysts to catalyze the

oxidation of various substrates by enzyme-generated hydrogen peroxide (H_2O_2) for colorimetric or fluorometric detection of acetylcholine and AChE inhibitors [14]. The most popular sensing configurations involve measurement of AChE inhibition with detection of the enzyme activity before and after exposure to pesticides.

Metallic nanoparticles -based sensors seem to be promising due to many unique properties that nanoscale materials offer. Among the different metallic nanoparticles, silver nanoparticles (AgNPs) possess many unique properties such as optical, mechanical, thermal and biological, compared to other metal nanoparticles, which make them attractive nanomaterials for uses in catalysis and sensing applications. Chemical reduction method is demonstrated to be the best method for the preparation of AgNPs due to the advantages of shape, and size control, easy formation and less time-consuming. The steps involved in the chemical reduction methods are reduction of silver nitrate using a reducing agent [15]. A variety of reducing agents have been used for preparation of AgNPs such as, using the juice extract of Citrullus lanatus (watermelon). The presence of polyphenol in this juice is found to be responsible for the reduction of Ag^{+1} to Ag^0 ions and also stabilization of AgNPs [16, 17]. AgNPs metallic nanocomposites show peroxidase- or oxidase-like activities. For instance, Au/Ag bimetallic nanoparticles promoted the H_2O_2-mediated oxidation for the fluorometric detection of acetylcholine [18].

Graphitic carbon nitride (g-C_3N_4) is also the most stable polymorphic analog of carbon nitride. In addition, because of its high nitrogen content, g-C_3N_4 can provide more active reaction sites than the other CN material and its lamellar structure benefits the transport of electron. g-C_3N_4 also excellent biocompatibility, high photoluminescence (PL) intensity [19] and good photostability properties. All of these unique characteristics make the g-C_3N_4 an ideal for bioimaging and chemical sensing [20], while only a few studies have been reported on its application in optical detection of environmental pollutant. For instance, it is applicable for fluorescence detection based on fluorescence quenching for Hg^{2+} [21], Cu^{2+} [22] and Fe^{3+} [23].

This research is focus on development of new technology known as nanotechnology based fluorometric biosensing method used for the detection of AChE and malathion. The key to this detection strategy is to make the AgNPs nanoparticle system sensitive by the modification of a suitable porous compound g-C_3N_4. The g-C_3N_4/AgNPs OFF-ON fluorometric biosensor is developed for detection of AChE extracted from young Catfish and ON-OFF for malathion in extracted from fresh Khat leaves.

EXPERIMENTAL

Chemical and Instruments

Siliver nitrate, sodium dihydrogen phosphate (98%), disodium hydrogen phosphate (98%), hydrochloric acid (England, 37%), urea (Poland, 98%), ethanol (absolute grade, 99%), Sodium hydroxide (BDH England, 98 %), potassium chloride and acetonitrile were used without purification. The instruments used were: Spectrofluorometer RF-5301pc (SCHIMADUZ, Japan), XRD (PANalytical X´Pert PRO-MPD diffractometer), FT-IR spectroscopy (PerkinElmer) and SEM-EDX (SEM Hitachi with EDX detector). The other apparatus included analytical balance (OHAUS, from Switzerland), oven (OV150C, from England), furnace (BiBBY, Stuart, from UK), hot plate (SM6, from UK), and deionizer (ELGACAN, Cartridge type C114, from UK), pH

meter (MP 220), sonicator, agate and pestle, crucibles, volumetric flasks, micropipettes, magnetic stirrer, measuring cylinder and beakers with different sizes were also used.

Preparation of juice extract

The Citrullus lanatus was collected from local market and washed with de-ionized water. It was cut into pieces. The inner red portion of the pieces was pasted by mortar pestle. Then, it was filtered using whatman filter paper to get Citrullus lanatus juice.

Synthesis of nanocomposites

About 5 mL of de-ionized water was added to 5 mL of pure juice extract to make it 1:1 and it was cooled in ice cold water. The solution was made alkaline (pH 10) by adding NaOH. The whole apparatus was placed on a heating mantle. During heating 6 mL 3 $x10^{-3}$ M aqueous silver nitrate solution was added drop wise with continuous stirring from burette and finally it was heated for 20 min at 70^0C. The color of the solution gradually changed from light pink to reddish yellow. The reddish yellow color indicated the formation of AgNP [24].

Graphitic carbon nitride (g-C_3N_4) was synthesized by pyrolysis of urea in a muffle furnace. 25 g (0.416 mol) urea was put into an alumina crucible with a cover, and it was heated up to 350^{o}C and then kept at this temperature for 1 h. Further heating was performed higher up to 500^{o}C and then kept at this temperature for 1 h. The heating rate of the whole reaction was 10^{o}C min^{-1}. Finally, 1 g of a yellow powder (g-C_3N_4) was collected.

The g-C_3N_4/AgNPs nanocomposite was synthesized by impregnation method. The g-C_3N_4 (0.1 g) was added to 30 mL of H_2O, and the suspension was stirred magnetically for 30 min and then sonicated for another 30 min. Then 2 mL AgNPs was added the above solutions and mixed under magnetic stirring and sonicated for 30 minutes. The resulting product was separated by centrifuging and washed three times with distilled water and ethanol and; the product was dried at 60^{o}C for 2 h. Finally, the g-C_3N_4/AgNPs product was collected and calcined in the muffle furnace at 300^{o}C for 1 h.

Morphological and structural characterization of the synthesized nanocomposites

The photoluminescence emission properties were determined using a RF-5301PC spectrofluorometer equipped with a xenon discharge lamp. The crystalline phases and the crystallite sizes was determined using powder X-ray diffraction (XRD) with X'Pert Pro PANalytical with CuKα radiation (λ = 1.5405 Å) and the surface morphology was determined by SEM-EDX (SEM Hitachi with EDX detector). The data were registered with 2θ steps of 0.02^o and accumulation times of 20 s. FT-IR (Spectrum 65, PerkinElmer) in the range 4000-400 cm^{-1} using KBr pellets was used to assign functional groups of as-synthesized g-C_3N_4/AgNPs.

Preparation of Buffers

The 0.1 M phosphate buffer was prepared by weighing approximately 0.8 g of $NaH_2PO_4.2H_2O$ and 6.5180 g of Na_2HPO_4 and dissolving them in water into a 500 mL volumetric flask. It was adjusted using 0.1 M HCl or 0.1 M NaOH to the desired pH. The buffer solution was stored in a fridge at 4^{o}C [25].

The 0.5M of Tris-HCl buffer was synthesized by dissolving 6.06 g of Tris base in 60 mL deionized water and adjust pH to 8 with HCl and diluted with deionized water to 100 mL and stored at 4^{o}C.

Extraction Methods

Ten young Catfish for extraction was collected from Haik Lake. It was acclimatized in 100 L aquaria for one week and then sacrificed by immersion in San ice bath (0℃). The brains was immediately removed, joined in pairs, and homogenized in 0.5 mol/L Tris-HCl buffer, pH 8, maintaining a ratio of 20 mg of tissue per mL of buffer using. The homogenates were centrifuged for 10 min at 1,000 g (4℃). After centrifuged the supernatants was collected from sample holder by needle in order to get active crude extracts from middle and the supernatants (crude extracts) was frozen at -20 ℃ [26].

Equal amount of milk and acetonitrile (8 mL each) was mixed and strongly shake for 1min. after a minute 2 mg of KCl salt was added and shaken for 1min. The result was centrifuged at 3000 rpm per 10 min and the supernatant was taken extract [27].

About 5 g of Khat leaf sample was also collected from south Wollo, Ethiopia for malathion extraction. The khat leaf was torn into very small pieces and ground using pistol and mortar. The powder was added into a flask that contains 15 to 20 mL of ethanol and sonicated for 15 minutes. The mixture was filtered through a buchner funnel to separate the liquid from the solid plant material and the liquid part was diluted by adding 5 mL of deionized water.

Detection of AChE in the presence of Substrate

The AChE-g-C_3N_4/AgNPs was prepared by dropping 30 μL of purified AChE solution (2 mg/mL) on to 2 mg of g-C_3N_4/Ag NPs and then 5 mL deionized water was added. The solution was continuing with stirring 30 min. About 1, 2, 4, 6, 8 and 10 mL of purified ACh was injected in to the cell containing AChE-g-C_3N_4/AgNPs and 10 mL sodium phosphate buffer (0.1 mol L^{-1}, pH 7.2) and sonicated. After reaction of 5 min at room temperature, the substrate (ACh) was enzymatically hydrolyzed to choline, which undergoes electrocatalytic oxidative. Therefore about 50 μL of the solution was taken into a cuvette and finally, the emission spectra were recorded using fluorescence spectroscopy.

Fluorescence Detection of Malathion

Fluorescence detection of malathion was performed according to the method described by researchers [28]. In a typical run, 2.5 mL of PBS (0.1 M, pH 7.2) was added into 5 mL of the AChE-g-C_3N_4/AgNPs, followed by the addition of different molar concentration of malathion, and sonicated. After reaction of 5 min at room temperature, 50 μL of the solution was taken into a cuvette and finally, the emission spectra were recorded using fluorescence spectroscopy.

In order to quantify the malathion induced quenching process, the Stern-Volmer quenching constant K_{SV} was calculated by Stern-Volmer equation:

$$I_O/I = 1+K_{SV}[Q] \quad (1)$$

Where I_O and I are the fluorescence intensities of the sensor in the absence and presence of malathion, respectively, K_{SV} is the Stern-Volmer constant and (Q) is the molar concentration of malathion.

Optimization of Parameters

The effect of pH (2-12) of PBS on the AChE-g-C_3N_4/AgNPs fluorescent biosensor in the presence of malathion solution was tested.

To study the effect of substrate concentration, different ACh concentrations, ranging from 100 to 1000 μM were used.

The effect of malathion concentration also affects the sensitivity of detection. In order to investigate this effect, 2.5 mL of PBS (0.1 M, pH= 6) was added in to the AChE/g-C_3N_4/AgNPs, followed by the addition of 100, 200, 300, 400 and 5000 μM of malathion solution and sonicated. After reaction of 5 min at room temperature, 50 μL of the solution was be taken into a cuvette and finally, the emission spectra were recorded using fluorescence spectroscopy.

Reproducibility and Stability Tests

The reproducibility of the AChE-g-C_3N_4/AgNPs as the fluorescent biosensor was investigated at three repetitions on three batches of the AChE-g-C_3N_4/AgNPs. A calibration graph was plotted for mean of F_O/F, (F_O and F represented the fluorescence intensity of sensor without and with malathion) vs. malathion concentration, which a linear range is then determined. Limit of detection was calculated using the following formula;

$$\text{LOD} = \frac{3\,x\,SD}{K_{SV}} \tag{2}$$

Where LOD are limit of detection, SD are standard deviation from linearity of a graph and K_{SV} is Stern-Volmer constant calculated from the graph [29].

Recovery Test and Real Samples Analysis

The resultant of extracted Khat samples was spiked with different concentrations of malathion solutions. Then 200 μL of this sample solution was taken and added to AChE-g-C_3N_4/AgNPs in 2.5 mL deionized water. Finally, fluorescence emission spectra were recorded after reaction of 5 min at room temperature.

The mean percentage recoveries for the malathion were calculated using the following equation:

$$\text{Percentage recovery} = \frac{CE}{CM}\ \text{X}\ 100 \tag{3}$$

Where CE is the experimental concentrations determined from the calibration curve and CM is the spiked concentrations.

RESULTS AND DISCUSSION

Characterization of the synthesized sensor

The XRD patterns of g-C_3N_4, AgNPs and g-C_3N_4/AgNPs nanocomposite are shown in Figure 1. The result indicate that the nanocomposite is well crystalline and reveals all diffraction peaks. It is observed that two diffraction peaks at 2θ value of 27.5° and 13.1° corresponding to the (002) and (100) diffraction planes respectively for g-C_3N_4, which is in good agreement with previous reports [30] (JCPDS 87-1526). The stronger peak at 27.5° corresponds to the interlayer stacking of the aromatic systems. The XRD analysis of biosynthesized AgNP to confirm the crystalline nature, it shows a characteristics peak at 31.81^0, 37.50^0, 44.10^0, 45.87^0, 56.58^0, 64.59^0 and 77.80^0. These indicate that the synthesized AgNP is crystalline and essentially fcc in nature. This result is a good agreement with other works [31].

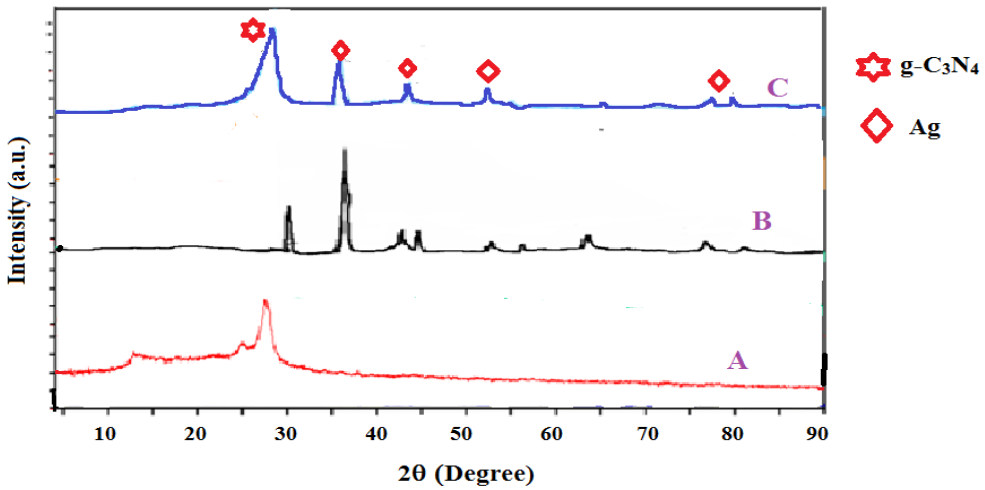


Fig. 1. XRD pattern of: a) g-C_3N_4, b) AgNPs, c) g-C_3N_4/AgNPs

For g-C_3N_4/AgNPs composites, the XRD patterns reveal a coexistence of both g-C_3N_4 and AgNPs. The presence of AgNPs nanoparticles onto g-C_3N_4 sheets might have resulted in disordered stacking of the nanocomposite. Therefore, the diffraction peak of g-C_3N_4/AgNPs slightly shifted compared to the pure nanoparticle, which may be attributed to the crystal lattice distortion in g-C_3N_4 due to the relatively strong interaction between the AgNPs. The diffraction peak is observed at 2θ values of 27.53º assigned to (002) plane due to g-C_3N_4 and 36.77º, 45.2º, 54.9º and 80.9º could be attributed to fcc AgNPs.

The developed nanocomposites were characterized by using the FT-IR technique to indicate functional groups as shown in Figure 2. The peaks at 1242, 1322 and 1413 cm^{-1} are typical stretching vibration modes of C=N and sp^3 C–N bond of heterocycles. There is also a characteristics band at 806 cm^{-1} attributed to the out-of plane breathing vibration characteristic of s-triazine units, these is in excellent agreement with samples of g-C_3N_4 produced from oxygenated precursors such as urea. For pure AgNP the FT-IR spectrum shows slightly narrower peak at 3458 cm^{-1} which may be due to hydroxyl (OH) stretching bands which suggests the involvement of the polyphenols in the reduction [32]. The peak around at 1600 cm^{-1} may be due to the presence of carbonyl group (C= O) associated with NH moiety in Riboflavin. The spectra for g-C_3N_4/AgNPs nanocomposite shows a peak at 3440 cm^{-1} are attributed due to hydroxyl (OH) stretching bands polyphenols of AgNPs. However, the AgNPs absorption peak was less noticeable, that may be attributed to the low content of AgNPs in the nanocomposites. The peaks are shifted to the lower wave numbers compared to pure nanoparticle. Furthermore, their intensities are changed after the Ag nanoparticles addition. The peaks of the g-C_3N_4 around 1600 cm^{-1} are shifted to 1579 cm^{-1}. These shifts of characteristic peaks of may be the result of the interactions between the g-C_3N_4 chains and AgNPs nanoparticles due to the formation of chemical bonding between the nanoparticle which contributes to charge transfer.

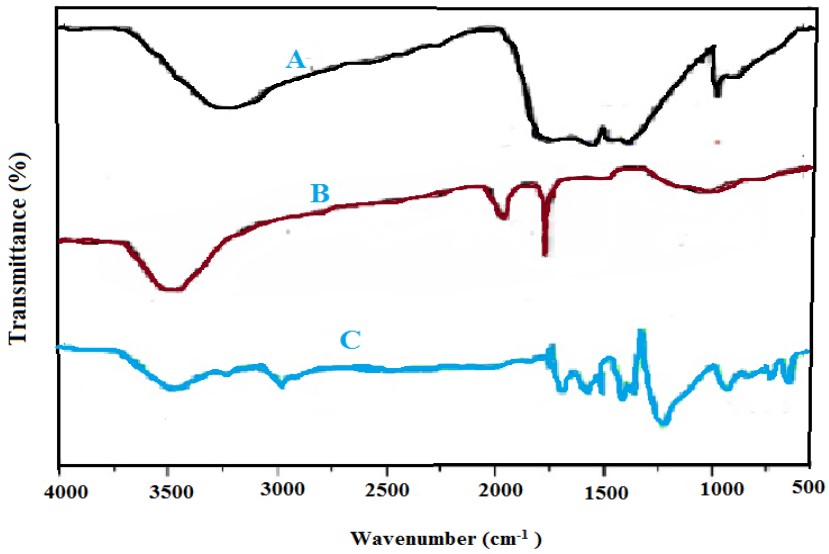


Fig. 2. FT-IR spectra of: a) g-C_3N_4, b) AgNPs, c) g-C_3N_4/AgNPs

Scanning electron microscopy (SEM) was used to analyze the morphological structure of the developed sensor sample. SEM images labelled as Figure 3a is for pure g-C_3N_4 has shown pores and layered structure. SEM analysis displays for AgNPs synthesized by watermelon extract are relatively spherical and uniform AgNPs was formed (Figure 3b).

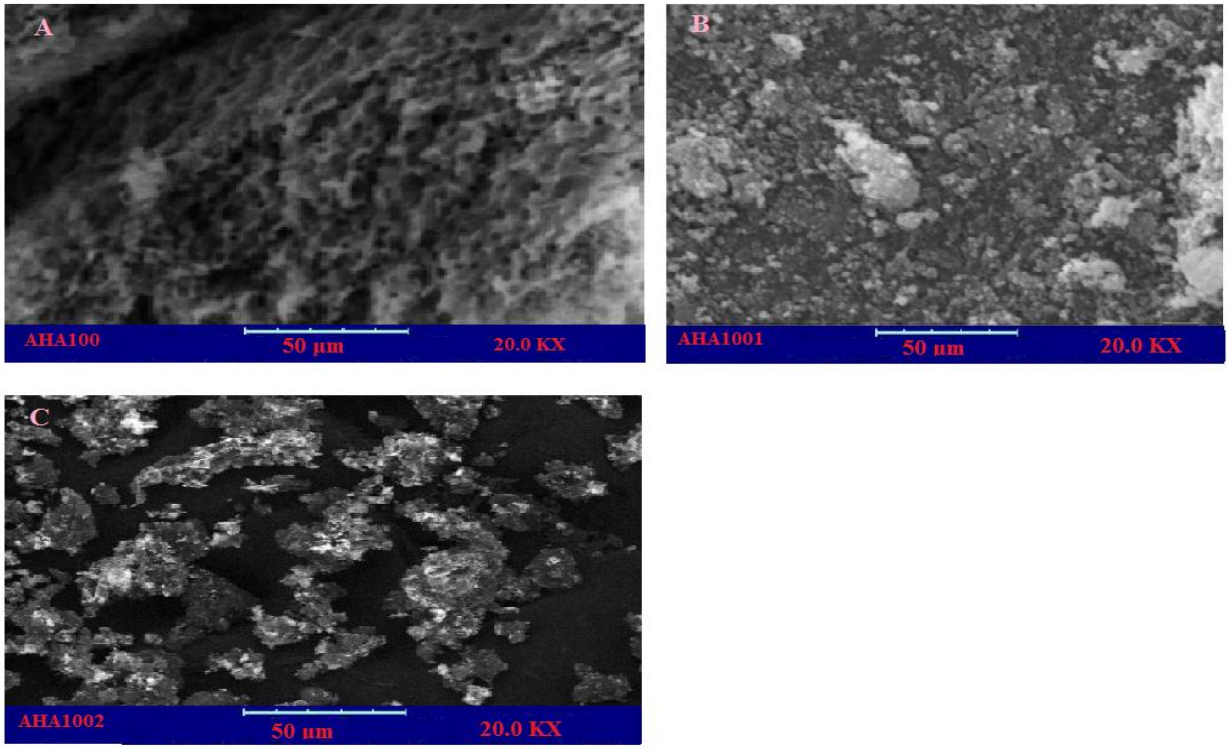


Fig. 3. Scanning electron microscopy analysis (SEM) of: a) g-C_3N_4, b) AgNPs, c) g-C_3N_4/AgNPs)

However, there are some aggregations are shown that may be due to the aggregation of smaller AgNps. Figure 3c describe the SEM analysis of g-C_3N_4/AgNPs, as clearly shown from the Figure the AgNPs is aggregate and deposited on the surface of g-C_3N_4 which confirms the existence of strong interaction between them.

Mechanism of g-C_3N_4/AgNPs Fluorescent Sensor for detection of Actylcholestrase (AChE) and Malathion

In order to investigate the performance of the g-C_3N_4/AgNPs for the detection of Actylcholestrase (AChE), the interaction between sensor sites and AChE were evaluated by the fluorescent intensity effect. The emission spectra were monitored at excitation wavelengths of 360 nm. After the addition of 1mL of purified ACh to the g-C_3N_4/AgNPs containing 10 mL sodium phosphate buffer (0.1 mol L^{-1}, pH 6). In the single enzyme system, AChE hydrolyzes acetylthiocholine to produce the thiocholine. In the bienzyme system, AChE catalyzes the hydrolysis of acetylcholine into acetate and choline which undergoes electrocatalytic oxidative. The reaction of thiocholine to g-C_3N_4 modified AgNPs through the formation of Ag and NH- of g-C_3N_4 forms bonds with ChO lead to the increase of fluorescence intensity of AChE−g-C_3N_4/AgNCs as shown in Figure 4. Therefore, the addition of AChE into the modified AgNPs resulted a "turn-on" fluorescent method or the intensity of fluorescence increases greatly due to several mechanisms such as the chelation-enhanced fluorescence and the yield of new fluorophore [33]. Generally, the fluorescent responses show an increase in intensity upon the additions of ACh as substrate. These results clearly indicated that a biosensor was established and that AChE as enzyme was hydrolyzing the substrate ACh, with the increase in oxidative electron as the preferred route of reaction.

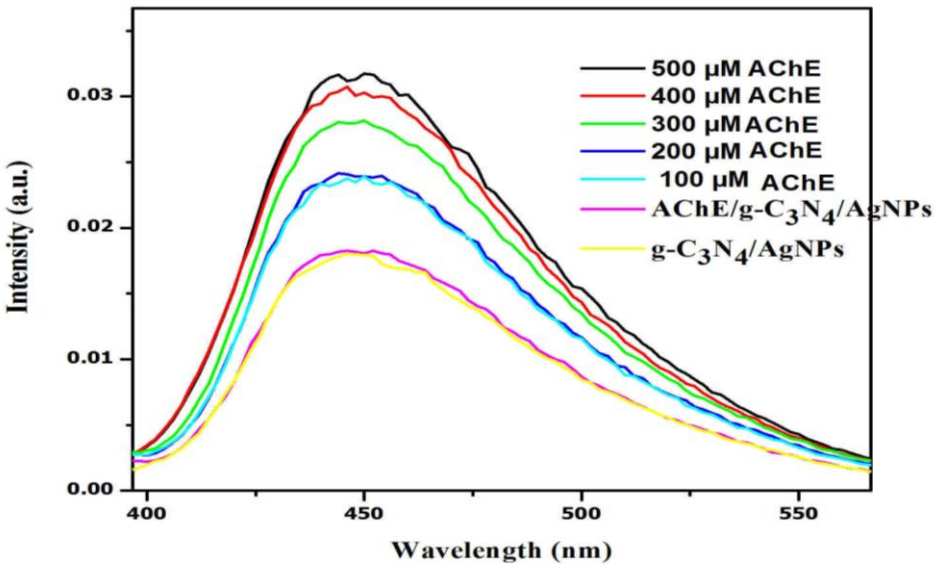


Fig. 4. Fluorescent detection of AChE

The development of new fluorophore AChE-g-C_3N_4/AgNPs have also been employed for organophosphorus pesticide (malathion) detection. The malathion pesticides prevented the production of thiocholine by inhibiting the activity of AChE, thus holding back the aggregation

of AgNPs on the surface of g-C_3N_4. It is also prevented the production of H_2O_2, resulting in a reduced catalytic oxidation of AgNPs and a decrease in the fluorescent intensity (quenching) as described in Figure 5. The other possibility for fluorescence intensity quenching occurs due to the most possible interactions between NH/N sites in g-C_3N_4/AgNPs with malathion would be like electrostatic or hydrogen bond for chelation (NH/N-O/S). This fluorescence static quenching indicates that fluorescence quenching is caused by chemical reactions.

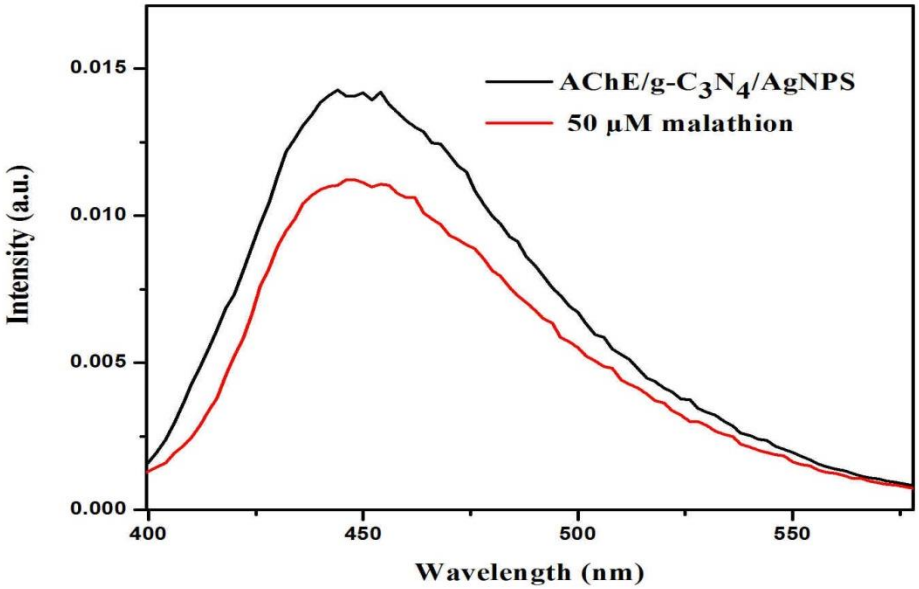


Fig. 5. Fluorescent detection of malathion by AChE-g-C_3N_4/AgNPs

Optimization of the AChE-g-C3N4/AgNPs fluorescent sensor

In order to evaluate the sensitivity of the proposed material, the experimental conditions were optimized including the pH of the buffer solution, concentration of acetylcholine (ACh) and malathion.

Solution pH also affects the performance of fluorescent intensity, so we examined the influence of pH on the fluorescent response of the sensor. The influence of pH on the quenching emission intensity of AChE-g-C_3N_4/AgNPs by malathion is described in Figure 6. The result indicated that a shift to lower intensity on turning with lower acidity, as well as the relative intensity ratio values decrease on going from pH 2 to pH 4. This is due to the fact that at lower pH both the interaction sites on AChE-g-C_3N_4/AgNPs and the malathion are fully protonated by H^+, resulting in a low quenching efficiency.

As the pH increased from 4 to 6, the fluorescence intensity significantly decreased due to the high quenching efficiency and maximum quenching was observed at pH 6. This is due to the deprotonation of the interaction site of AChE-g-C_3N_4/AgNPs, which increases the covalent bond strength between the sensor and malathion. As the pH further increases pH >6, due to competitive hydroxide formation, it resulted in a distinct increase in fluorescence intensity resulting in a poor interaction with the sensor. These results indicated that AChE-g-C_3N_4/AgNPs is applicable to detect the malathion in a weak acidic and neutral condition. Therefore, pH 6 is recommended as the optimal pH value for further detection.

The effect of purified ACh on the biosensor response was studied by varying the concentration from 100-1000 µM. There was a linear relationship between the biosensor response/immobilized AChE activity and ACh concentration. Based on these results, 1mM was selected as the optimum concentration in subsequent experiments.

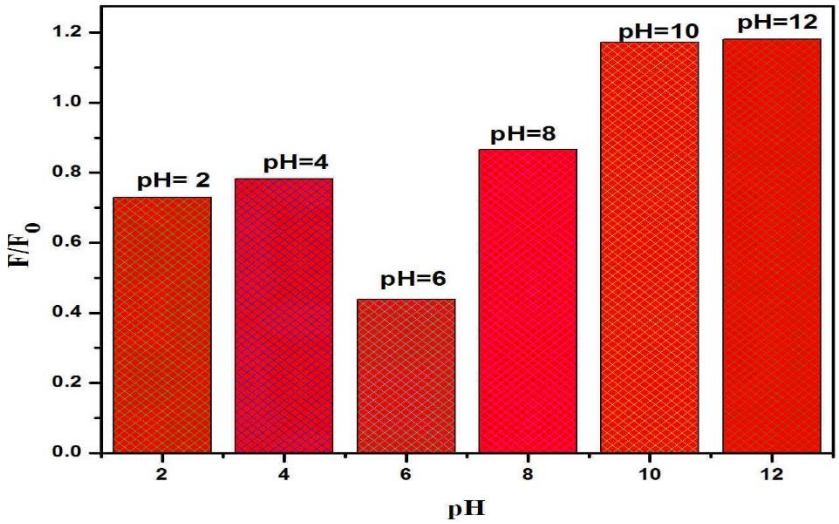


Fig. 6. Effect of pH

The changes in the emission spectra of AChE-g-C_3N_4/AgNPs was followed upon addition of different concentrations of malathion as described in Figure 7. The fluorescence intensity is quenching upon addition of these malathion analytes. As described in the mechanism above (section 3.2) this is due to the properties of malathion forming a reaction at surface of the AChE-g-C_3N_4/AgNPs, so that resulting in electron transfers..

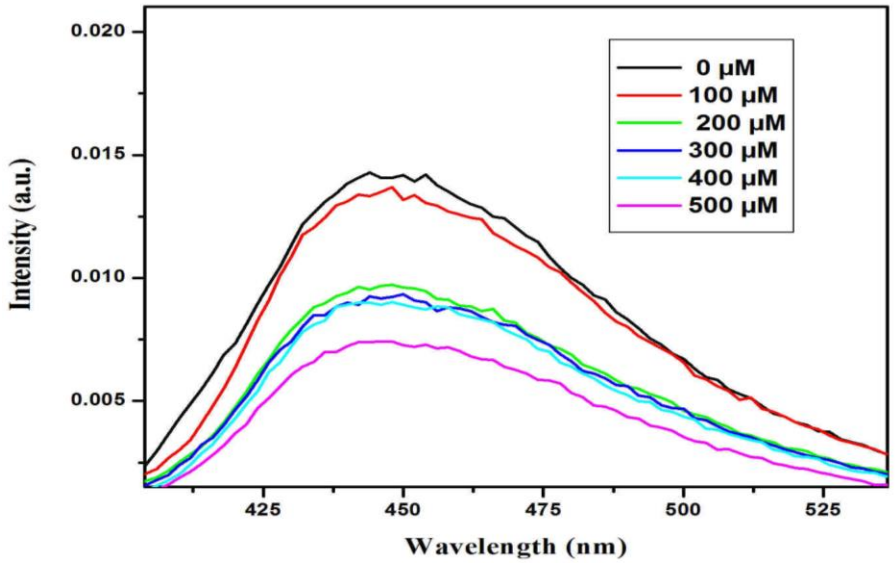


Fig. 7. Emission spectrum of AChE-g-C_3N_4/AgNPs upon addition of malathion with various concentration

Additionally, the reason is due to cross-linking/aggregation of interparticle occurs because of the electrostatic interaction between thiocholine and citrate on g-C_3N_4/AgNPs surface. The prominent feature is that the intensity of emission is gradually quenched with an increase in the concentration of these malathion in aqueous solution. Nevertheless, the fluorescence quenching test indicates, a higher concentration of malathion, there is no more quench the fluorescence intensity of the as-synthesized fluorometric biosensor thoroughly; as the concentration was increased to from 100- 500 μM, the fluorescence quenching was observed clearly and the fluorescence intensity therefore decreases linearly. Therefore, 500 μM is the optimum concentration of malathion

Sensitivity of the Detection System

The high sensitivity of the developed AChE-g-C_3N_4/AgNPs sensor at pH 6, suggests possible application of the developed fluorometric biosensor method for analysis of Malathion. The fluorescence intensity of the developed sensor was found to be such that quenching and the Stern-Volmer fluorescence intensity ratio (F_O/F) show a linear diminish with the increasing malathion concentration from 100 μM to 500 μM as described in Figure 8. The fluorescence titration experiments showed the malathion concentration is inversely proportional to fluorescence intensity, and gave a good linear change in Stern-Volmer fluorescence emission intensity ratio.

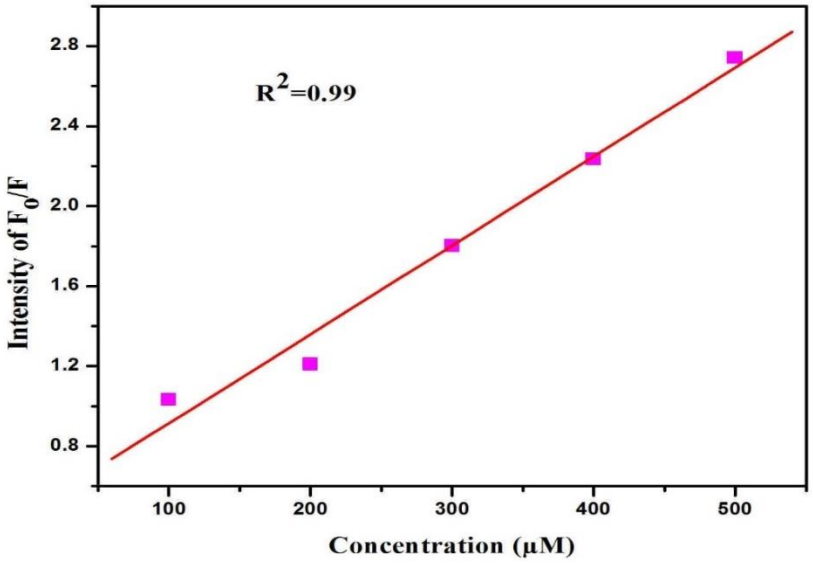


Fig. 8. The reproducibility of the AChE-g-C_3N_4/AgNPs responses for malathion concentration

In order to clarify the favorable condition for the AChE-g-C_3N_4/AgNPs to interact with the malathion, quenching efficiency at excitation wavelength was determined using a Stern-Volmer plot (eqn 1). In a fluorescent biosensor, the emission intensity ratio can be defined as the response of the sensor. The sensing capability of the AChE-g-C_3N_4/AgNPs was revealed from the slopes of the linear plots, which were corresponding to the quenching rate constants (K_{SV}). A linear relationship with the coefficients of regression of R^2= 0.99 was obtained at the concentration ratio of the probe. The sensitivity of determination is directly related to the K_{SV} value. Therefore,

the calculated K_{SV} value for the AChE-g-C_3N_4/AgNPs fluorescent biosensor for detection of malathion was found to be $3.48x10^{3}$ M^{-1}.

In order to determine the LOD of the AChE-g-C_3N_4/AgNPs fluorescent biosensor, the reproducibility of the developed sensor at the linear range was investigated at three repetitions. The LOD of the AChE-g-C_3N_4/AgNPs for the malathion determined from the standard deviation of the response at the intercept of the regression line and the value of the K_{SV} (eqn 2). Therefore, the limit of detection of the proposed fluorescent biosensor for malathion was found to be 9.807×10^{-5} M. The detection limit in this case was also good compared with those of the other fluorophore based fluorescent sensing methods as described in table 1.

Table 1. *Comparing of the performance of the sensor*

Sensing material	Linear range	LOD	Reference
AChE/DDAO	___	4.0×10^{-5} M	[34]
RB-AuNPs	__	0.3 μg/L	[35]
AChE-g-C_3N_4/AgNPs	100-500 μM	9.807×10^{-5} M	This work

Recovery test

The Khat samples collected from south Wollo, Ethiopia was spiked with different concentration of malathion solutions. From the calibration curves plotted for the known standard solution (spiked) of malathion, the unknown (found) concentration of malathion (value of X) was successfully calculated by using equation y = A + B*X obtained from the calibration curves of the standard solution. In this case, the value of "A" is intercept and B (slope) and the value of y (F_O/F) was obtained from the fluorescence recorded for malathion for khat samples. The result indicated a good linear relation between F_O/F and the spiked concentrations of malathion with coefficient of regression $R^2 = 0.979$ as described in Figure 9.

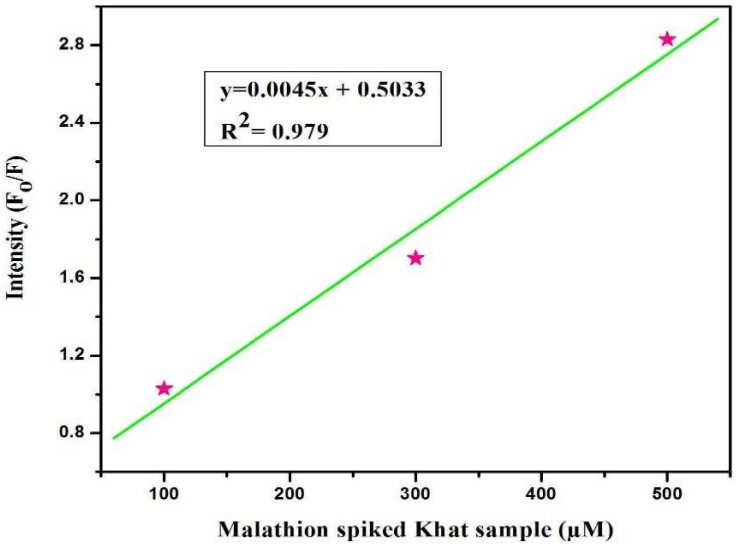


Fig. 9. Calibration curve of F_O/F Vs. different concentration of malathion spiked khat sample

The calculated results were summarized in table 2, and it could be seen that the found values is agreed well with the spiked amount. The obtained recoveries in such samples varied from 95.4% to 106.8 %, which demonstrates that the proposed method is valid and denoting no serious interferences in the samples. As well, the RSD were less than 5 %, suggesting a high precision of the proposed method.

Table 2. *Detection of malathion in khat samples by spiked method (n = 3)*

Samples	Added (μM)	Found (μM)	Mean recovery (%) a	RSD (%)
Khat				
1	100	106.8	106.8	1.8
2	300	286.4	95.4	1.09
3	500	517	103.4	0.6
	Unknown	168.8		

Detection of malathion in Khat Samples at optimized condition

In this study, under optimizing all parameters (pH, 6: 1 mM of ACh), khat samples used in this work contain a detectable amount of malathion as shown in Figure 10. This suggests that AChE-g-C_3N_4/AgNPs fluorescent biosensor has a promising prospect for the detection of malathion in real samples. The calculated amount of malathion concentration in Khat sample was found to be 168.8 μM. This may be due to possible reasons for high level of malathion.

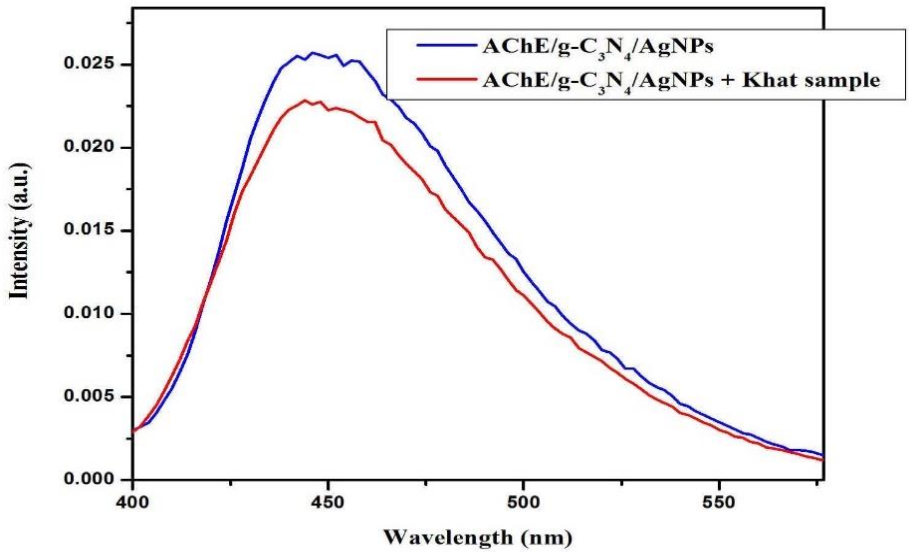


Fig. 10. Fluorescence emission spectra of AChE-g-C_3N_4/AgNPs with Khat samples

The reason is most farmers in these areas use malathion as pesticide to protect khat from disease and pests. Besides human exposure, there is also concern that these pesticides could leak into ground and municipal water supplies and pollute surrounding environment. Malaoxon is an oxygen analogue of malathion and it can be found either as an impurity in malathion product, or can be generated during the oxidation of malathion in air or soil.

CONCLUSIONS

AChE-g-C_3N_4/AgNPs was developed by covalent immobilization on g-C_3N_4/AgNPs modified nanocomposite. Thus, covalent coupling between enzyme and nanocomposite material was very efficient for retaining the activity of immobilized AChE and preventing it from leaking out of the biosensor AChE biosensor. The as-synthesized fluorescent biosensor utilized as a highly effective tool for selective AChE and malathion detection. The detection of malathion present in aqueous solution was based on quenching in the emission intensities resulting from complex formation of the sensor molecule with malathion, and this malathion effectively quenched the emission intensity of AChE-g-C_3N_4/AgNPs. The detection of malathion by nitrogen-containing and noble Ag NPs fluorophores suggests that the distinct types of optical responses observed in present AChE-g-C_3N_4/AgNPs can be explained as having a high surface-area-to-volume ratio and exposes all its coordination points to the detected analyte. The developed sensor exhibited a linear range, a high sensitivity with a low detection limit of 9.807 x 10^{-5} M. This study is important because it can provide us environmentally friendly fluorescent probes for rapid, highly sensitive optical detections of malathion by enzyme modulated probe.

Acknowledgment

I would like to express my deepest appreciation and thanks to Department of Chemistry, Wollo university for instruments and laboratory facilities as well as for facilitating required stuffs from the beginning to the completion of this work. I would like thank my friend Temam Gemeda for extraction of Actylcholestrase from fish. I would like also thanks Addis Ababa University for providing spectroscopic analysis

Source of Funding

This research did not receive any specific grant from funding agencies in the public, commercial, or not-for-profit sectors.

REFERENCES

1. FEPA (The Federal Environmental Protection Authority). 2004. Environmental Impact Assessment Guideline on Pesticides. FEPA, Addis Ababa, Ethiopia.
2. Chen, C., Qian, Y., Chen, Q., Tao, C. and Li, C. 2011. Evaluation of pesticide residues in fruits and vegetables from Xiamen, China. *Food Control*, 22: 1114–1120.

3. Ariese, F., Ernst, W.H.O. and Sijm, D.T. 2001. Natural and synthetic organic compounds in the Environment a symposium report. *Environmental Toxicology and Pharmacology*, 10: 65-80.
4. Ebrahima, S., El-Raeyb, R., Hefnawya, A., Ibrahimb, H., Solimana, M., and Abdel-Fattah T.M. 2014. Electrochemical sensor based on polyaniline nanofibers/single wall carbon nanotubes composite for detection of Malathion. *Synthetic Metals*, 190:13–19.
5. Andreescu, S. and Marty, J.L. 2006. Twenty years research in cholinesterase biosensors: From basic research to practical applications. *Biomolecular Engineering*, 23: 1–15.
6. Pohanka, M. 2014. Inhibitors of acetylcholinesterase and butyrylcholinesterase meet immunity. *International Journal of Molecular Sciences*, 15: 9809–9825.
7. Pedrosa, V.A., Caetano, J., Machado, S.A.S. and Bertotti, M. 2008. Determination of parathion and carbaryl pesticides in water and food samples using a self assembled monolayer/acetylcholinesterase electrochemical biosensor. *Sensors*, 8: 4600-4610.
8. Sukirtha, T.H. and Usharani, M.V. 2013. Gas chromatography-mass spectrometry determination of organophosphate pesticide residues in water of the irrigation canals the North Zone, Tamil Nadu/India. *International Journal of Current Microbiology and Applied Science*, 2(8): 321-329.
9. Guan, H., Brewer, W. E. and Garris, S. T. 2010. Disposable pipette extraction for the analysis of pesticides in fruit and vegetables using gas chromatography/mass spectrometry. *Journal of Chromatography A*, 1217: 1867-1874.
10. Petropoulou, S.S.E., Gikas, E., Tsarbopoulos, A. and Siskos, P.A. 2006. Gas chromatographic–tandem mass spectrometric method for the quantitation of carbofuran, carbaryl and their main metabolites in applicators' urine. *Journal of Chromatography A*, 1108(1): 99-110.
11. Delmulle, B.S., De Saeger, S.M., Sibanda, L., Barna-Vetro, I. and Van Peteghem, C.H. 2005. Development of an immunoassay-based lateral flow dipstick for the rapid detection of aflatoxin B1 in pig feed. *Journal of Agricultural and Food Chemistry*, 53(9): 3364-3368.
12. Kalele, S.A., Kundu, A.A., Gosavi, S.W., Deobagkar, D.N., Deobagkar, D.D. and Kulkarni, S.K., 2006. Rapid detection of Escherichia coli by using antibody-conjugated silver nanoshells. *Small*, 2(3): 335-338.
13. Zhou, H.K., Gan, N., Hou, J.G., Li, T.H. and Cao, Y.T. 2012. Enhanced electrochemiluminescence employed for the selective detection of methyl parathion based on a zirconia nanoparticle film modified electrode. *Analytical Sciences*, 28: 267–273.
14. Liang, M., Fan, K., Pan, Y., Jiang, H., Wang, F., Yang, D., Lu, D., Feng, J., Zhao, J. and Yang, L. 2013. Fe_3O_4 magnetic nanoparticle peroxidase mimetic-based colorimetric assay for the rapid detection of organophosphorus pesticide and nerve agent. *Analytical Chemistry*, 85: 308–312.
15. Ahmad, B.M., Lim, J.J., Shameli, K., Ibrahim, N.A. and Tay, M.Y. 2011. Synthesis of silver nanoparticles in chitosan, gelatin and chitosan/gelatin bionanocomposites by a chemical reducing agent and their characterization. *Molecules*, 16(9): 7237-7248.
16. Maiti, S., Barman, G. and Konar Laha, J. 2014. Biosynthesized Gold nanoparticles as catalyst. *International Journal of Scientific and Engineering Research*, 5(7): 1229-1230.
17. Huang, X., Wu, H., Liao, X. and Shi, B. 2010. One-step, size-controlled synthesis of gold nanoparticles at room temperature using plant tannin. *Green Chemistry*, 12(3): 395-399.
18. Wang, C.I., Chen, W.T. and Chang, H.T. 2012. Enzyme mimics of Au/Ag nanoparticles for fluorescent detection of acetylcholine. *Analytical Chemistry*, 84: 9706–9712.

19. Huang, H., Chen, R., Ma, J., Yan, L., Zhao, Y., Wang, Y., Zhang, W., Fan, J. and Chen, X. 2014. Graphitic carbon nitride solid nanofilms for selective and recyclable sensing of Cu^{2+} and Ag^{+} in water and serum. *Chemical Communications*, 50(97): 15415- 15418.

20. Lee, E. Z., Jun, Y. S., Hong, W. H., Thomas, A. and Jin, M. M. 2010. Cubic mesoporous graphitic carbon (IV) nitride: An all-in-one chemosensor for selective optical sensing of metal ions. *Angewandte Chemie International Edition*, 49: 9706- 9710.

21. Zhuang, Q., Sun, L. and Yongnian, N. 2017. One-step synthesis of graphitic carbon nitride nanosheets with the help of melamine and its application for fluorescence detection of mercuricions. *Talanta*, 164: 458-462.

22. Tian, J., Liu, Q., Asiri, A. M., Al-Youbi, A.O. and Sun, X. 2013. Ultrathin graphitic carbon nitride nanosheet: a highly efficient fluorosensor for rapid, ultrasensitive detection of Cu^{2+}. *Analytical Chemistry*, 85: 5595-5599.

23. Zhang, S., Li, J., Zeng, M., Xu, J., Wang, X. and Hu, W. 2014. Polymer nanodots of graphitic carbon nitride as effective fluorescent probes for the detection of Fe^{3+} and Cu^{2+} ions. *Nanoscale*, 6(8): 4157- 4162.

24. Maiti, S., Barman, G. and Laha, J.K. 2016. Detection of heavy metals (Cu^{+2}, Hg^{+2}) by biosynthesized silver nanoparticles. *Applied Nanoscience*, 6(4):529-538.

25. Bisetty, K., Sabela, M.I., Khulu, S., Xhakaza, M. and Ramsarup, L. 2011. Multivariate optimization of voltammetric parameters for the determination of total polyphenolic content in wine samples using an immobilized biosensor. *International Journal of Electrochemical*, 6: 3631-3643.

26. Assis, C.R., CASTRO, P.F.and Bezerra, R.S. 2010. Characterization of acetylcholinesterase from the brain of the amazonian tambaqui (colossoma macropomum) and in vitro effect of organophosphorus and carbamate pesticides. *Environmental Toxicology and Chemistry*, 29(10): 2243–2248.

27. Anastassiades, M., Lehotay, S.J., Stajnbaher, D and Schenich, F.J. 2003. Fast and easy multi residue method employing acetonitrile extraction/partitioning dispersive and solidphase extraction for the determination pesticides residue in produce. *Journal of AOAC International*, 86(2): 412-418.

28. Yang, C., Wang, X., Liu, H., Ge, S., Yu, J. and Yan, M. 2017. On–off–on fluorescence sensing of glutathione in food samples based on a graphitic carbon nitride (g-C3N4)–Cu^{2+} strategy. *New Journal of Chemistry*, 41(9): 3374-3379.

29. Alim, N.S., Lintang, H.O. and Yuliati, L. 2015. Fabricated metal-free carbon nitride characterizations for fluorescence chemical sensor of nitrate ions. *Journal Technologi (Sciences & Engineering)*, 76 (13): 1-6.

30. Ye, L., Liu, J., Jiang, Z., Peng, T. and Zan, L. 2013. Facets coupling of BiOBr-g-C_3N_4 composite photocatalyst for enhanced visible-light-driven photocatalytic activity. *Applied Catalysis B: Environmental*, 142: 1-7.

31. Maiti, S., Barman, G. and Konar Laha J. 2016. Detection of heavy metals (Cu^{+2}, Hg^{+2}) by biosynthesized silver Nanoparticles. *Applied Nanoscience*, 6:529–538.

32. Song. J.Y., Jang H.K. and Kim, B.S. 2009. Biological synthesis of gold nanoparticles using Magnolia kobus and Diospyros kaki leaf extracts. *Process Biochemistry*, 44(10):1133–1138.

33. Kim J.S. and Quang D.T. 2007. Calixarene-derived fluorescent probes. *Chemical Review*, 107: 3780–3799.

34. Zhang, Y.; Hei, T.; Cai, Y.; Gao, Q.; Zhang, Q. 2012. Affinity binding-guided fluorescent nanobiosensor for acetylcholinesterase inhibitors via distance modulation between the fluorophore and metallic nanoparticle. *Analytical Chemistry*, 84: 2830–2836.

35. Liu, D.; Chen, W.; Wei, J.; Li, X.; Wang, Z.; Jiang, X. 2012. A highly sensitive, dual-readout assay based on gold nanoparticles for organophosphorus and carbamate pesticides. *Analytical Chemistry*, 84: 4185–4191.